

ANALYSIS AND STRUCTURAL INVESTIGATIONS ON NEOLITHIC PAINTED POTTERY FROM ZĂUAN “DÂMBUL SPÂNZURAȚILOR” ARCHAEOLOGICAL SITE

ANAMARIA CARSTEA (ELEKES)¹, MIHAI GLIGOR¹, IOAN ALIN BUCURICA^{2,*},
IOANA DANIELA DULAMA^{2,*}, CRISTIANA RADULESCU^{3,4,5},
RALUCA MARIA STIRBESCU², ANDREEA LAURA BANICA^{2,4},
SORINA GEANINA STANESCU²

Manuscript received: 11.12.2024; Accepted paper: 16.04.2025;

Published online: 30.06.2025.

Abstract. In this study, archaeometric investigations of ancient pottery were conducted, a topic that has gained importance in recent decades. In this regard, a batch of ten painted ceramic samples from two types of features discovered at Zăuan - Dâmbul Spânzuraților: domestic and funerary in order to be analysed and to provide scientifically proven information given by archaeometric methods for the identification of materials and production techniques, the origin and provenance, involving the characterization and location of natural sources of raw materials used in different types of archaeological ceramic pieces, clay sources, firing temperatures, and decorative motifs.

Keywords: Neolithic pottery; Herpály culture; ICP-MS; FTIR; optical microscopy; statistical analysis.

1. INTRODUCTION

The Neolithic painted pottery of northwestern Transylvania has been enriched with new assemblages in the last years based on the new archaeological research carried out in Sălaj County at Zăuan-Dâmbul Spânzuraților.

The site Zăuan-Dâmbul Spânzuraților is located on the left terrace of the Barcău River situated in the geographic area called the Sylvania Depression (Fig. 1). It is well known since the last century, from the 80's, when the first archaeological researches were carried out, on which occasion two pits G1, G2 and part of a sunken dwelling were identified and investigated [1]. These three complexes brought to the surface archaeological materials which proved the existence of a Neolithic community in this area assigned to the Herpály culture, a community which until that date had not been attested in the territory of Sălaj County [2-5].

¹ 1 Decembrie 1918 University of Alba Iulia, 510009 Alba Iulia, Romania. E-mail: carstea_r@yahoo.com; mihai.gligor@uab.ro.

² Valahia University of Targoviste, Institute of Multidisciplinary Research for Science and Technology, 130004 Targoviste, Romania. E-mail: stirbescu.raluca@icstm.ro; banica.andreea@icstm.ro; geanina.stanescu@icstm.ro.

³ Valahia University of Targoviste, Faculty of Sciences and Arts, 130004 Targoviste, Romania. E-mail: cristiana.radulescu@valahia.ro.

⁴ National University of Science and Technology Politehnica of Bucharest, Doctoral School Chemical Engineering and Biotechnology, 060042 Bucharest, Romania.

⁵ Academy of Romanian Scientists, 050044 Bucharest, Romania.

* Corresponding author: bucurica_alin@icstm.ro; dulama.ioana@icstm.ro.

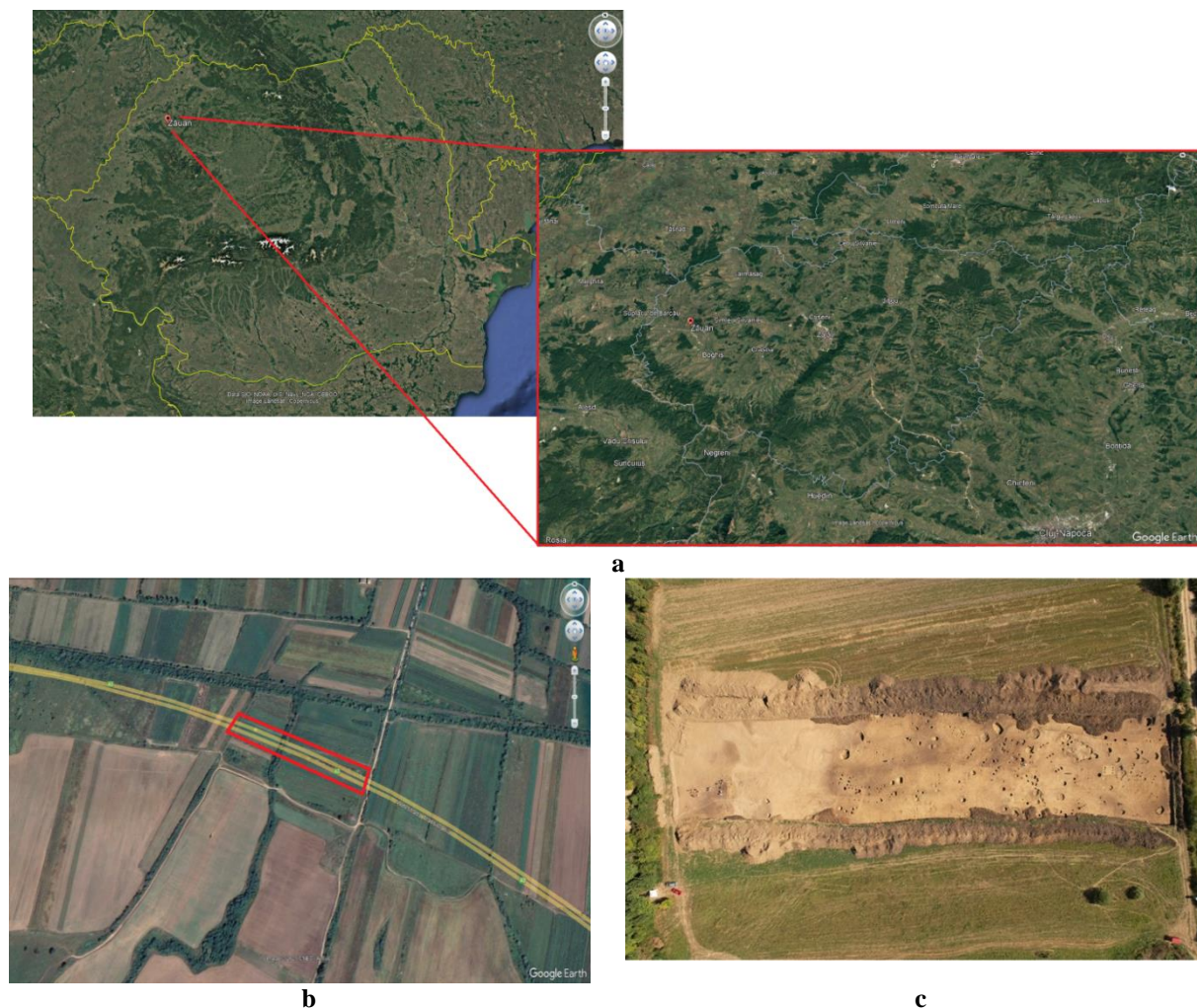


Figure 1. Archaeological site: a) Location of Zăuan in Romania (left side) and Sălaj County (right side); b) Zăuan – Dâmbul Spânzuraților, area surveyed in 2021; c) area S2/2021 with surveyed complexes.

Although the first reference to a settlement in this area is found by K. Miklós, who collected materials from Zăuan “Kétvizközt” and “Dâmbul Cimitirului” which appeared as a result of agricultural works between 1963-1974 [6], the first research campaign was carried out in 1975 and aimed to know the stratigraphy and chronology of the site. Later, research areas were opened that had the role of researching previously identified complexes. In all the 4 systematic research campaigns (1975, 1976, 1977, 1980), 2 sections, 5 quadrants, totaling an area of 243 m² were drawn [1, 7].

Excavations carried out until now at *Dâmbul Spânzuraților* proved the fact that the whole geographic area was inhabited by communities beginning with those belonging to the Starčevo-Criș, Pișcolt, Herpály, Tiszapolgár, and continuing with Coțofeni and Cehăluț attributed to the Bronze period [2]. Unfortunately, such materials were not identified in systematic research, which would have allowed to observe the relations between the last stages of development of the Starčevo-Criș communities and the following cultural groups with painted pottery from the northwest of Romania [8].

If the first researches were carried out on the plateau area of the terrace, the archaeological research carried out in 2020 for the Transylvania Motorway indicated that the settlement is much more extensive and includes also the low area of the Barcău river terrace. In 2021, archaeological researches were carried out at this point, totaling approximately 14,000 square meters, 389 features being researched, most of them attributed to the Herpály culture. Based on the type of features, the various sizes of the pits, the surface structures -

possible annexes, as well as certain characteristics of their inventory (a large part of the pits being full adobe, sometimes large pieces of wall) we considered that we were in a peripheral area of the *Dâmbul Spânzurașilor* settlement, and only one of the Herpály features could have had the functionality of a dwelling. Five of the features represented inhumation graves (another grave in which were identified cremated remains was assigned to this category after the anthropological analysis was finished), located among pits and other surface structures - possible annexes [4].

2. MATERIALS AND METHODS

2.1. MATERIALS

Neolithic communities from the Sylvanian Depression are the creators of a very aesthetic, elegant, painted pottery, which is distinguished by its plasticity and variety of assortment. The majority of the pottery is represented by coarse ware with a brown, brown-grayish colour with sand or gravel in a small amount in composition as temper. The category of fine or semifine ware, with tempers that consist of very fine sand, micas, and ceramoclast, or silt, has a brown, brown-grayish color, or more rarely yellowish grey or reddish-yellow surface. In this category can also find black and brown-black colour.

The thickness of the vessel walls also varies in the case of fine and semi-fine ware from 3 mm to 10 mm thick. The main categories of the vessels that are to be found in this case are: biconical vessels (bowls), hemispherical vessels (bowls, cups), vessels with a globular body (bowls, pots), "amphorae", pedestal vessels, miniaturals ones, lids, and "unusual" shapes such as pot holders. Cups are preponderant in number, the bowls are also present in large numbers and generally have a hemispherical body, conical bowls or with slightly arched walls, and vessels with slightly oblique walls that are almost straight. Jars fragments are fewer in number, the pedestal forms are well represented as well: cups and bowls with high stems.

The painted decoration consists mostly of wide or narrow strips, with black color found only on fine or semifine sherds, and consists of fine lines to simple black bands arranged on the surface of the vessel, emphasizing parts of the pot like the rim, knobs, or the entire body. Generally, painted decoration is to be found mostly on open shapes and consists of parallel strips that altogether form geometric shapes, wide angular bands, narrow bands, or lines parallel to the rim, vertical strips arranged on the body of the vessel or on the pedestal, narrow bands with meandering motifs, and hatched bands. On very few vessels is preserved the black colored layer used as decoration, on several is preserved only its marks.

As a decorative motif, incisions can also be observed on the rim of the vessels or on the surface, consisting of paralleled straight lines that form right angles. Also, knobs are to be observed on the upper part of the bowls, pots.

The typology and ornamentation of painted pottery from Zăuan – *Dâmbul Spânzurașilor* can certainly prove that this type of artefact shows remarkable aesthetic and technological characteristics.




Pottery discovered during the archeological excavations carried out in this area has already been published [1, 2, 5], but researches were limited to description and presenting the stratigraphy in general. There is very little information about the chemical composition of the pottery and only a few studies on the painted decoration, which is characteristic to the Neolithic pottery in this area. Until now, only identification and composition analysis of the






black material used on decorated archeological ceramics found at the Porț “Corău” site had been published. The results of these analyses concluded that the decoration is organic, being a mixture of birch bark tar with natural bitumen [9].



Although the latest results of archaeometric analysis carried out on a batch of ceramic pieces from the same archeological site, Suplacu de Barcău/Port “Corău”: optical microscopy, scanning electron microscopy coupled with energy dispersive spectrometry (SEM-EDS) and attenuated total reflectance Fourier transform infrared spectroscopy (ATR-FTIR), give us a larger point of view about the technical methods of manufacturing ceramics in the Neolithic. Based on the obtained results in terms of the firing temperature, the elemental content of the pottery was also established. In this regard, it can be concluded that the source of the clay was local, and the ceramics were made locally from the same material. Also, a major conclusion of the investigations was that the 11 samples studied confirm that the pottery from different archaeological features does not show major differences either in terms of composition of the paste, the manufacturing process, or the method of decoration [10].

In order to be able to establish the chemical composition of the pottery, the origin of raw materials, and the technology used by the Neolithic communities, a total of ten ceramic fragments from the Zăuan-Dâmbul Spânzuraților site were analyzed (Table 1). The fragments are painted using a black colour and the decoration is well-preserved on some parts, but on others, only the trace of the decoration is preserved.

Table 1. Ceramic samples – details about archaeological context and images.

S (the number of the trench)	Cx (context)	▼ (depth) [m]	Inventory number	Sample No. (short presentation)
S2/2021	191 /2021 inhumation grave	-0.80-0.96	275/2022	 <p>Sample 1 (Herpály type pottery) - Fine ceramic vessel rim fragment with painted decoration marks.</p>
S2/2021	347 /2021 inhumation grave	-0.80-1.30	516/2022	 <p>Sample 2 (Herpály type pottery) - Fine ceramic vessel rim fragment with painted decoration marks.</p>
S2/2010	24 /2021 inhumation grave	-0.80-1.10	122/2022	 <p>Sample 3 (Herpály type pottery) - Fine ceramic vessel rim fragment with painted decoration marks.</p>

S (the number of the trench)	Cx (context)	▼ (depth) [m]	Inventory number	Sample No. (short presentation)
S2/2021	60/2021 inhumation grave	-0.80	526/2022	 <p>Sample 4 (Herpály type pottery) - Fine ceramic fragment with painted decoration marks.</p>
S2/2021	271/2021 pit	-0.80 -1.52	487/2022	 <p>Sample 5 (Herpály type pottery) - Fine ceramic fragment with painted decoration.</p>
S2/2021	87 pit	-0.80-1.20	189/2022	 <p>Sample 6 (Herpály type pottery) - Fine ceramic fragment with painted decoration.</p>
S2/2021	27/2021 pit	0.80 – 1.17	129/2022	 <p>Sample 7 (Herpály type pottery) - Fine ceramic vessel rim fragment with painted decoration marks.</p>
S2/2021	253/2021 pit	0.90 -1.96	465/2022	 <p>Sample 8 (Herpály type pottery) - Fine ceramic vessel rim fragment with painted decoration marks.</p>

S (the number of the trench)	Cx (context)	▼ (depth) [m]	Inventory number	Sample No. (short presentation)
S2/2021	11/2021 pit	0.80-1.40	75/2022	 <p>Sample 9 - (Herpály type pottery) - Fine ceramic vessel rim fragment with painted decoration and protuberance.</p>
S2/2021	199/2021 pit	0.80-1.42	292/2022	 <p>Sample 10 (Herpály type pottery) - Fine ceramic vessel incised rim fragment with painted decoration and pierced.</p>

Four clay samples (i.e., 1-4) were collected from the site (Table 2). Clay samples were collected from the archaeological excavations. It was not possible to gather samples from the surroundings because is already been built a highway there. All the samples come from section S2; the first sample was collected from feature Cx 198C, which was identified as a clay pit. Cx 347 and Cx 298 were inhumation graves, and the last one was also a pit (Cx115).

Table 2. Clay samples - details about archaeological features from Zăuan - Dâmbul Spânzurașilor.

Sample	S - the number of the trench/the archaeological campaign; Cx - context
Soil_1	S2/2021, Cx 198C – clay pit
Soil_2	S2/2021, Cx 347 – inhumation grave
Soil_3	S2/2021, Cx 298 – inhumation grave
Soil_4	S2/2021, Cx 115 - pit

As a decorative motif, incisions can also be observed on the rim of the vessels or on the surface, consisting of paralleled straight lines that form right angles. Also, knobs are to be observed on the upper part of the bowls, pots.

2.2. METHODS

The analytical techniques used for physicochemical investigation (i.e., optical microscopy – OM, attenuated total reflectance-Fourier transform infrared spectroscopy – ATR-FTIR, and inductively coupled plasma mass spectrometry – ICP-MS) allowed a complex characterization of Zăuan – *Dâmbul Spânzurașilor* painted pottery.

2.2.1. Optical microscopy

For the analysis of the samples, the Zeiss Stemi-2000c microscope coupled with the Zeiss Axiocam 105 camera was used for image acquisition and Zen software for processing (all are produced by Zeiss, Oberkochen, Germany). The magnification factor used was 6.5X in order to obtain descriptive information of the samples and to observe aspects relevant to further investigations.

2.2.2. Attenuated total reflectance-Fourier transform infrared spectroscopy

The ten ceramic and four soil samples were analyzed using a Vertex 80 FTIR spectrometer (Bruker, Berlin, Germany) coupled to a Hyperion 2000 high-resolution microscope (Bruker, Berlin, Germany). The attenuated total reflectance module (ATR), equipped with a diamond crystal and platinum tip, was used; 32 scans per sample were set in the range 400-4000 cm^{-1} .

2.2.3. Inductively coupled plasma mass spectrometry

Ceramic (separated into two subsamples: #B – black pigment and #R - background) and soil samples were digested using aqua regia according to the specifications presented in Table 3 using the TopWave digestion system (Analytic Jena GmbH, Jena, Germany). The digested samples were transferred to volumetric flasks and diluted to 50 mL with ultrapure water [11].

Table 3. Digestion procedure (recipe and program) for soil and ceramic samples.

Sample type	Sample mass [g]	Flask [mL]	Used reagents	Reagent volume [mL]	Temperature [°C]	Pressure [bar]	Time [min]	Power [%]
Soil	0.400	50	HNO ₃	2.5	180	40	25	80
Pottery	0.050		HCl	7.5				

The multielemental content (i.e., Mg, Al, K, Cr, Mn, Fe, Ni, Co, Cu, Zn, Cd, In, and Pb) of painted pottery and blank solutions was measured using an iCAPTM Qc mass spectrometer (Thermo Scientific, Darmstadt, Germany) in the standard mode. For all samples, the measurements were collected in triplicate, and the reported data are the mean values (with $\text{RSD} \leq 5.24\%$); the Qtegra Intelligent Scientific Data Solution software (Thermo Scientific, Darmstadt, Germany) has allowed to removal of some well-known interferences. The calibration curve was chosen as the quantification method (the calibration curves were obtained utilizing ICP multi-element standard solution IV, produced and commercialized by Merck, Darmstadt, Germany), and the blank solutions were used to calculate the limits of detection (LOD) and quantitation (LOQ) for the proposed method (Table 4). The ICP-MS method was verified using 2710a Montana I Soil standard reference material (National

Institute of Standards and Technology, Gaithersburg, Maryland, USA) with a recovery level in the range of 97-103%.

Table 4. NIST SRM 2710a certified and measured data (expressed as mg/kg), as well as the LOD and LOQ values (expressed as µg/kg).

	SRM 2710a certified [mg/kg]	SRM 2710a measured [mg/kg]	Recovery [%]	LOD [µg/kg]	LOQ [µg/kg]
Cd	12.300 ± 0.300	12.445 ± 0.466	101	0.129	0.143
Cu	0.342 ± 0.005	0.348 ± 0.025	101	1.185	1.476
Ni	8.000 ± 1.000 (<i>rv*</i>)	7.811 ± 0.548	97	0.662	0.793
Pb	0.552 ± 0.003	0.540 ± 0.042	97	1.211	1.292
Mn	0.214 ± 0.006	0.222 ± 0.009	103	1.384	1.933
Zn	0.418 ± 0.015	0.409 ± 0.020	97	0.733	0.863
Fe	4.32 ± 0.08	4.332 ± 0.191	100	1.366	1.447

*rv** means reference value

2.2.4. Statistical analysis

The potential correlations between the elemental content of the studied samples (ceramic and soil samples) were assessed by Pearson correlations and hierarchical cluster analysis using the IBM SPSS Statistics 26 program (Armonk, NY: IBM Corp). This part is essential for highlighting the potential source of clay for the ancient pottery.

3. RESULTS AND DISCUSSION

The optical microscopy highlighted the presence of the pigments applied on ceramics as well as the structural density of the fragments subjected to the study. Furthermore, the presence of some unusual shapes or models was pinpointed along with cracks, striations, inclusions, or eventually detached minerals. All these aspects are approached one by one in this chapter.

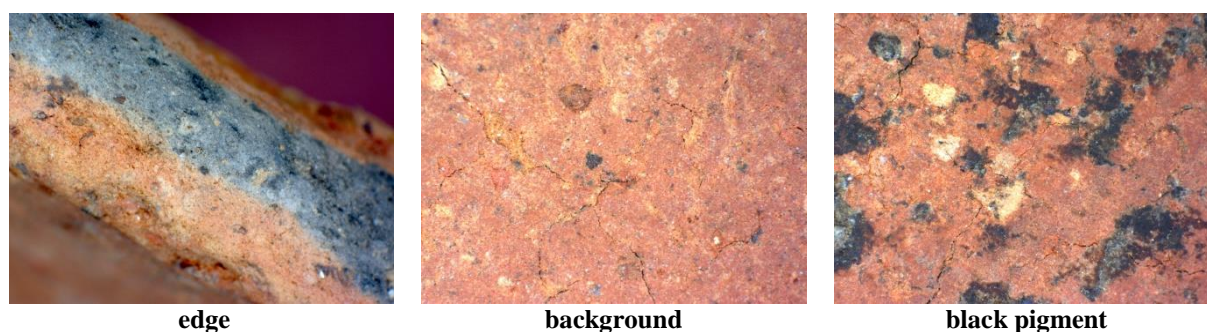


Figure 2. Sample 1 - Optical microscopy (6.5X).

Sample 1 was presented with a relatively compact structure, gray and reddish on the edge, and visible cracks on the front side. The predominant color is reddish, which is quite common in ceramics, and inserts of possible pigments in the form of black spots. The surface texture does not seem to be very smooth and highlights several aspects related to the execution and manufacturing process of the ceramics.



Figure 3. Sample 2 - Optical microscopy (6.5X).

Sample 2 has an apparently not very dense texture of reddish color on the edges of the edge but black throughout the central area. The sample shows fine cracks on the lateral surface, without mechanical striations and with a few fine cracks. In terms of flatness, the surface shows noticeable unevenness. A few black spots, possibly pigment, were also observed. The sample does not show material dislocations.

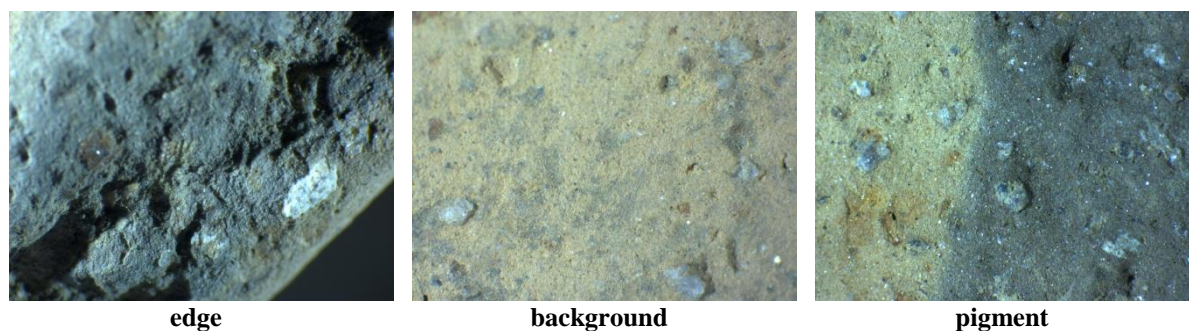


Figure 4. Sample 3 - Optical microscopy (6.5X).

Sample 3 is cream-colored on the sides and gray on the edges. In addition, on the front side is visible an ornament consisting of a black pigment in the form of a curved line and a dot. Regarding the structure of the material, the ceramic is presented in a compact and dense form, without visible cracks or striations. Some material removals can also be observed on the side face; however, in general, the sample shows a fine roughness, placing it among the samples with the smoothest surface of those studied



Figure 5. Sample 4 - Optical microscopy (6.5X).

The background of sample 4 is cream-reddish and has a relatively large, uneven but quite compact grain. No cracks are visible, only material displacements, and on the edge, along with the predominant color referred to above, the black color applied as a possible pigment or resulting from burning is also distinguished. The surface covered with pigment appears much flatter and smoother than the natural background.



Figure 6. Sample 5 - Optical microscopy (6.5X).

The structure of sample 5 looks a bit different than the previous ones but quite dense, and as for its color, the ceramic has a mixture of black and cream-brown on one side, while on the other side, it is black with shades of gray. The edge is predominantly black and has some fine cracks similar to the ones on the lateral surface background. It appears as a uniform ceramic, which may be due to the firing duration during the manufacturing process. On one side, the ceramic presents shades of gray-black colors arranged in a sort of pattern, which makes it difficult to identify as a stencil.

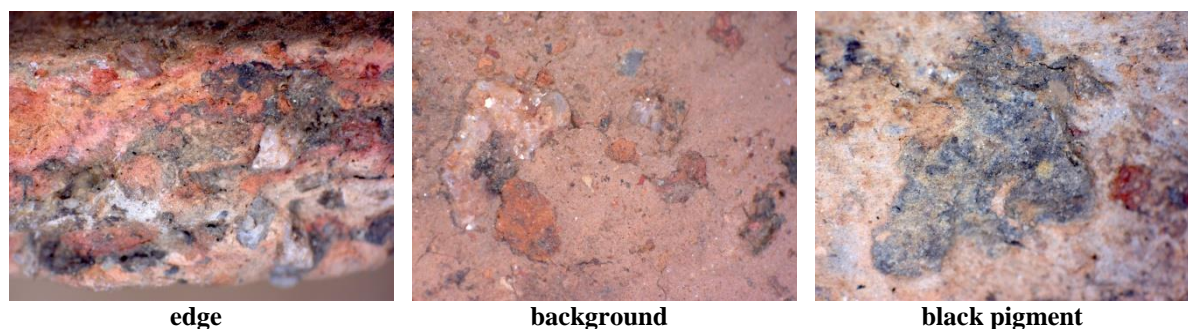


Figure 7. Sample 6 - Optical microscopy (6.5X).

Visually, in the case of ceramic sample 6, a large grain and a variation of colors that include white, red, gray, black, cream, or brown, as well as different minerals, can be distinguished along the edge. The background is provided by a cream-brown color on one side and a reddish-brown color on the other, over which a pigment has been applied, in the form of a coloristic template consisting of transverse and longitudinal black lines. The coarse but fairly compact structure can be observed both in the case of the image showing the background and in the case of the one in which the black pigment can be observed. Cracks are present but are not of notable size.

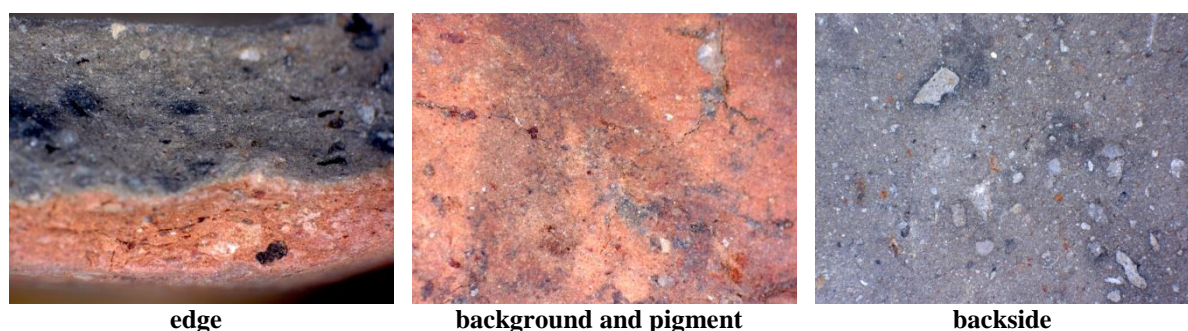


Figure 8. Sample 7 - Optical microscopy (6.5X).

The ceramic samples investigated by optical microscopy presented some interesting visual aspects, and sample 7 also has some peculiarities. The image depicting the edge

contains two main colors: black and red. On one side, there is a pattern featuring black stripes. No cracks were present.

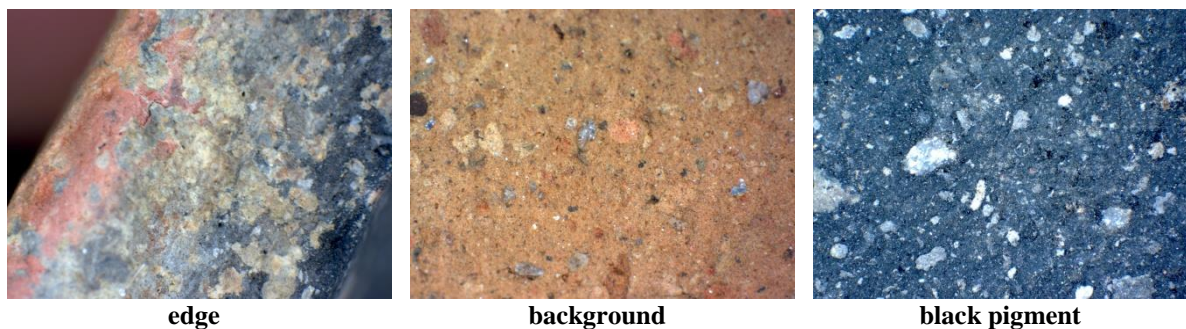


Figure 9. Sample 8 - Optical microscopy (6.5X).

Sample 8 has a reddish color with black portions (possibly pigment). On the edge, both the red and black areas are covered with distinguished gray spots. It is a sample with a homogeneous-grained texture. No cracks are noticeable. Sample 9 has a brown-cream color with black spots and a relatively large protuberance on one side, while the other side is completely black. It is a homogeneous and fine-grained sample. Among the analyzed samples, it can be distinguished as the sample with the finest texture. There is no pattern when it comes to color; there are no visible stripes like in other cases, nor cracks in the material.



Figure 10. Sample 9 - Optical microscopy (6.5X).

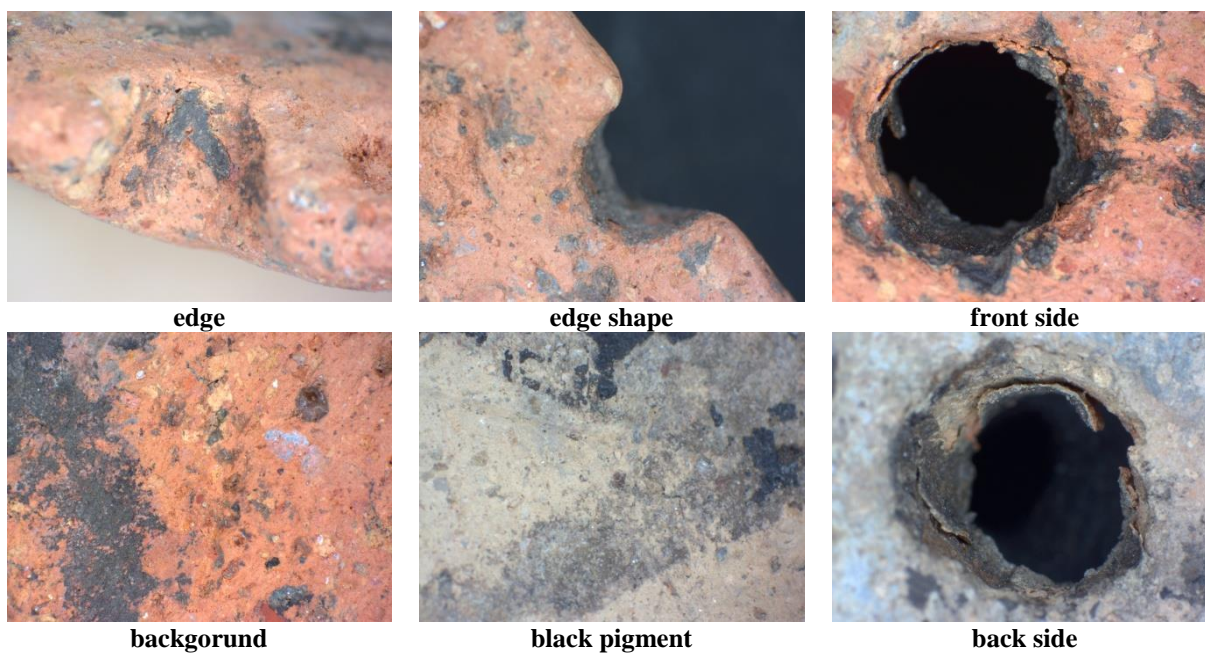


Figure 11. Sample 10 - Optical microscopy (6.5X).

Sample 10 was a rather interesting sample due to its complexity. A constructive pattern is observed on the edge that includes several circular shapes and a hole near the center. On the front side is visible an ornament constituted from some black pigment stripes. The sample does not show any noticeable cracks.

Ancient ceramics often contained organic and inorganic compounds, which were identified using ATR-FTIR spectroscopy, well known as a non-invasive analytical technique [12-16]. In the mid-infrared spectral range ($4000-400\text{ cm}^{-1}$), the fingerprint peaks and band assignment were examined (Tables 5 and 6). On background subsamples, the weak band $1629-1645\text{ cm}^{-1}$ (corresponding to CO_3^{2-} bending) and the weak peak of $1432-1442\text{ cm}^{-1}$ (CO_3^{2-} stretching), together with the weak bands at $718-719\text{ cm}^{-1}$ show the presence of calcite in the analyzed samples.

Table 5. Infrared absorption peaks of analyzed background subsamples with relative intensity (s=strong, m=medium, w=weak) and tentative assignment (ν =stretching vibration; δ =bending vibration).

Background subsamples	IR peaks [cm^{-1}]									
	444-452	516-518	641-645	692-693	718-719	777-778	796-797	994-1036	1432-1442	1629-1645
#1R	s			w		w	w	s		w
#2R	w	w		w		w	w	s	w	w
#3R	w		w	w	w	w	w	s		w
#4R	w	w		w		w	w	s		w
#5R	w			w		w	w	s	w	w
#6R	s		w	w	w	w	w	s		w
#7R	s	w		w		w	w	s		w
#8R	s		w	w		w	w	s		w
#9R	s		w	w		w	w	s		w
#10R	m			w		w	w	m		w
Tentative assignment	$\nu(\text{Si-O})$	$\delta(\text{Si-O-Al}) / \delta(\text{O-H-Fe-O})$	$\delta(\text{O-H-Al}) / \delta(\text{O-H-Mg})$	Si-O-Al	$\delta(\text{CO}_3^{2-})$	$\nu(\text{Si-O})$	$\nu(\text{Si-O})$	$\nu(\text{Si-O}) / \nu(\text{Si-O-Al})$	$\nu(\text{CO}_3^{2-})$	$\nu(\text{C-C}) / \delta(\text{CO}_3^{2-})$

Several silicates, including kaolinite and muscovite, were identified in the background subsamples, in addition to calcite. These compounds were identified as the source of the Si-O-Al/Si-O stretching or bending vibrations for which the main bands are around $994-1036\text{ cm}^{-1}$, $692-693\text{ cm}^{-1}$, $516-518\text{ cm}^{-1}$, and $444-452\text{ cm}^{-1}$. The Si-O stretching vibration in quartz was identified as the cause of the $796-797\text{ cm}^{-1}$ and $777-778\text{ cm}^{-1}$ weak peaks (samples #1R – #10R), while the Al-OH bond in kaolinite was identified by the strong peaks at $994-1036\text{ cm}^{-1}$ (all samples except #10R, characterized by a medium peak). The weak peaks located between 641 and 645 cm^{-1} were attributed to bending or deformation vibrations of OH groups that are directly bonded to aluminum and/or magnesium from smectite (identified in subsamples #2R, #4R, and #7R). Similar results were reported by Tamilarasi and Chandrasekaran in their study [17].

Table 6. Infrared absorption peaks of analyzed black pigment subsamples with relative intensity (s=strong, m=medium, w=weak) and tentative assignment (v=stretching vibration; δ = bending vibration).

Black pigment subsample	IR peaks [cm^{-1}]									
	447-453	568	635-646	692-694	718-723	777-778	796-797	992-1056	1430	1629-1634
#1B	s			w		w	w	s		w
#2B	s			w		w	w	s	w	w
#3B	s		w	w		w	w	s		w
#4B	s		w	w	w	w	w	s		w
#5B	s			w		w	w	s		w
#6B	s			w		w	w	s		w
#7B	s			w		w	w	s		w
#8B	s			w		w	w	s		w
#9B	s		w	w	w	w	w	s		w
#10B	m	w	w	w		w	w	m		w
Tentative assignment	v(Si-O)	$\delta(\text{PO}_4^3)$	$\delta(\text{O-H-Al})$ / $\delta(\text{O-H-Mg})$	Si-O-Al	$\delta(\text{CO}_3^{2-})$	v(Si-O)	v(Si-O)	v(Si-O)/ v(Si-O-Al)	v(CO_3^{2-})	v(C-C)/ $\delta(\text{CO}_3^{2-})$

On the black pigments, the weak band $1629\text{--}1634\text{ cm}^{-1}$ (corresponding to CO_3^{2-} bending) and the weak peak of 1430 cm^{-1} (CO_3^{2-} stretching, in the case of #2B sample), together with the weak bands at $718\text{--}723\text{ cm}^{-1}$ (#4B and #9B samples) shows the presence of calcite in the analyzed samples. As in the case of background subsamples, the Si–O–Al/Si–O stretching or bending vibrations were observed: $992\text{--}1056\text{ cm}^{-1}$, $692\text{--}694\text{ cm}^{-1}$, and $447\text{--}453\text{ cm}^{-1}$. In the same time, the quartz presence was identified in all samples ($796\text{--}797\text{ cm}^{-1}$ and $777\text{--}778\text{ cm}^{-1}$ bands), while smectite was identified in four samples (#3B, #4B, #9B, and #10B). In sample #10B, a weak signal was observed at 568 cm^{-1} , corresponding to the mineral calcium apatite.

The IR data are very important to estimate the firing temperature (Table 7) by the presence or absence of some mineral phases [18]. In this step, the quartz and feldspar can not be used because they are minerals that do not depend on the firing temperatures [19]. However, the kaolinite's presence suggests a firing temperature below 650°C [12]. If the hematite band ($\sim 535\text{ cm}^{-1}$) is observed, the firing temperature was more than 600°C , while the band around 875 cm^{-1} represents a firing temperature over 800°C [17, 20, 21]. According to this information, the firing temperature of the analysed samples (taking into account the background subsample) was estimated. In this respect, all studied samples were obtained by firing in an oxidizing atmosphere, at temperatures lower than 600°C (Table 7).

Table 7. Determination of the firing temperature according to representative IR bands.

Sample	875 cm^{-1} band	T_{875} [$^\circ\text{C}$]	535 cm^{-1} band	T_{535} [$^\circ\text{C}$]	Kaolinite bands		$T_{\text{kaolinite}}$ [$^\circ\text{C}$]	Estimated firing temperature [$^\circ\text{C}$]
					1025 cm^{-1}	440-460 cm^{-1}		
#1R	no	<800	no	<600	yes	yes	<650	<600
#2R	no	<800	no	<600	yes	yes	<650	<600
#3R	no	<800	no	<600	yes	yes	<650	<600
#4R	no	<800	no	<600	yes	yes	<650	<600
#5R	no	<800	no	<600	yes	yes	<650	<600
#6R	no	<800	no	<600	yes	yes	<650	<600
#7R	no	<800	no	<600	yes	yes	<650	<600
#8R	no	<800	no	<600	yes	yes	<650	<600
#9R	no	<800	no	<600	yes	yes	<650	<600
#10R	no	<800	no	<600	yes	yes	<650	<600

The ICP-MS results obtained following the method described in section 2.2.3 are presented in Table 8. The preliminary observation of the elemental content, it possible to distinguish the elements that can be used to differentiate the black pigment from the background subsamples. It is well known that in the Neolithic, pottery decorations were made from the same clay, but adding different coloured soils (washed until a fine powder was obtained) [22].

Table 8. Elemental content in pottery and soil samples (expressed as mg/kg, except aluminum expressed as %) and the mean relative standard deviation (expressed as %).

	Mg	Al	K	Cr	Mn	Fe	Ni	Co	Cu	Zn	Cd	In	Pb
#1B	304.28	6.48	338.38	209.00	82.88	1074.92	165.87	5.46	17.50	30.46	0.23	0.06	11.91
#1R	200.93	4.37	203.98	190.07	90.27	968.06	165.04	5.57	8.35	17.94	0.14	0.04	8.86
#2B	309.17	5.26	210.01	163.97	99.27	864.59	178.89	2.01	3.67	25.32	0.62	0.15	10.37
#2R	113.94	3.98	167.22	76.03	52.13	390.76	114.21	1.97	2.07	14.54	0.23	0.05	10.27
#3B	315.34	3.03	138.45	117.34	77.04	664.92	194.66	4.49	7.19	20.13	0.15	0.04	7.42
#3R	439.73	3.80	253.71	157.24	346.28	877.30	118.90	10.75	6.92	26.59	0.53	0.08	9.72
#4B	169.75	7.00	201.54	108.86	71.55	582.81	155.14	2.20	1.89	20.57	0.54	0.07	10.43
#4R	119.16	4.19	179.58	79.40	56.37	425.58	126.33	1.68	2.07	18.23	0.23	0.05	9.94
#5B	192.81	3.65	236.80	136.32	118.11	1124.17	161.21	4.74	6.69	42.34	1.70	0.10	16.81
#5R	141.38	5.35	196.33	103.87	62.56	513.67	148.57	2.66	2.25	18.01	0.46	0.08	10.43
#6B	339.07	5.35	327.23	175.64	142.51	840.16	116.89	4.30	15.65	26.08	0.26	0.04	9.85
#6R	365.34	5.02	318.42	170.15	130.31	976.63	131.85	4.70	16.62	25.85	0.18	0.05	9.20
#7B	305.55	4.35	170.86	183.24	225.72	838.13	133.55	8.01	13.39	21.06	0.24	0.04	8.52
#7R	290.67	6.14	233.10	148.94	278.37	966.91	140.48	7.05	9.39	23.44	0.19	0.04	8.32
#8B	207.83	8.99	204.64	112.97	83.50	666.83	175.86	1.58	3.38	23.69	0.46	0.05	10.35
#8R	334.47	3.24	154.28	141.63	84.77	737.89	108.25	5.24	8.16	23.14	0.19	0.04	8.38
#9B	380.51	3.75	197.40	185.80	407.68	882.68	131.24	11.18	17.07	30.99	0.26	0.03	12.47
#9R	408.42	4.53	232.47	133.29	81.99	969.47	129.70	4.64	12.68	32.83	0.24	0.04	11.10
#10B	120.88	4.48	189.08	93.18	61.63	456.10	140.74	1.41	2.72	16.10	0.31	0.02	9.80
#10R	655.30	10.62	391.58	225.16	228.07	1591.00	229.46	12.70	14.10	86.49	0.36	0.07	12.43
Soil_1	268.14	3.34	205.37	222.74	68.33	270.01	32.76	2.30	2.93	28.92	1.06	0.34	15.59
Soil_2	323.08	4.05	240.03	122.71	50.18	325.48	37.77	2.69	3.02	30.31	1.05	0.14	17.74
Soil_3	274.31	3.20	191.44	270.33	80.70	261.91	31.42	2.07	3.43	34.79	1.32	0.20	15.21
Soil_4	295.13	3.64	222.36	171.93	54.25	292.27	36.29	2.41	3.03	27.82	1.19	0.11	16.55
Mean RSD [%]	3.71	2.23	5.01	2.86	5.24	3.16	2.94	2.79	2.65	2.15	2.45	2.03	2.93

The analyzed pottery samples are characterized by: Al and Fe as major constituents, Mg, K, Cr, and Ni as minor constituents, while Mn, Co, Cu, Zn, Cd, In, and Pb as trace elements. The variations between background and black pigment subsamples are the most important characteristics in the elemental analysis due to the information about the coloured soils added to the clay.

The main observation about the major constituent is related to the small amount in soil samples compared with the pottery subsamples. At the same time, the content in black pigment was higher than the content in the background subsamples in the case of #1, #2, #4, and #5 for iron as well as #1, #2, #4, #6, and #8 for aluminum. Another important element for the pigment analysis is manganese, which, together with iron, is responsible for the brown-black colour of painted pottery. In our case, the manganese was higher in the pigment than the background subsample in the case of #2, #4, #5, #6, and #9. However, taking into account the deterioration degree of the painting on the pottery, it can be concluded that the coloured soils used for the black pigment were rich in iron and manganese [23].

The second observation on ICP-MS data is related to Ni, Co, and Cu; for those elements, the content in almost all pottery subsamples was higher than the content in soil samples. On the other hand, Cd, In, and Pb have recorded higher values in soil samples than

in pottery subsamples. According to the elemental content of analyzed samples, it can be determined the potential clay sources, if the site was the center of pottery production or not, as well as the nature of decorations (i.e., black pigment). In this respect, the statistical analysis was performed based on ICP-MS results.

Factor analysis is a statistical method used to explain the variability among observed and correlated variables based on a smaller number of unobserved variables (factors). The content of the 13 elements was subjected to principal component analysis (PCA) to reveal the structural links between the elements (i.e., Mg, Al, K, Cr, Mn, Fe, Ni, Co, Cu, Zn, Cd, In, and Pb) identified in the ceramic pigments subjected to analysis. The Kaiser-Meyer-Olkin (KMO) test and Bartlett's test of sphericity are shown in Table 9, while the anti-image matrix is presented in Table 10. Those analyses were used to evaluate the correlations between the obtained data on the principal component analysis (Table 11 and Fig. 12).

Table 9. KMO and Bartlett's Test.

Kaiser-Meyer-Olkin Measure of Sampling Adequacy		0.654
Bartlett's Test of Sphericity	Chi-squared test ($\sim\chi^2$)	225.204
	Degree of freedom (df)	78
	Significance (Sig.)	<0.001

The KMO value recorded for the 20 analyzed black pigment subsamples was 0.654, which indicates an acceptable level and suggests the significant existence of correlations between variables [24]. In the case of the Bartlett test, the obtained values present a significant level with $\chi^2 = 225.204$, $df = 78$, and $p = < 0.001$. These two items (KMO and Bartlett test) confirm that the original materials used for the black pigments present similarities from a chemical point of view. Table 10 presents the values obtained from the correlations of the analyzed samples for the 13 elements determined. The Measure of Sampling Adequacy (MSA) was applied because the values obtained on the table diagonal indicate the suitability of each variable for inclusion in the PCA analysis [25].

In order to highlight the links between the elements determined in all pottery subsamples and to simplify the data, the principal component analysis (PCA) was performed. This method allows for a direct and clear presentation of the data for the 13 variables (chemical elements: Mg, Al, K, Cr, Mn, Fe, Ni, Co, Cu, Zn, Cd, In, and Pb).

Table 10. Measure of Sampling Adequacy.

	Mg	Al	K	Cr	Mn	Fe	Ni	Co	Cu	Zn	Cd	In	Pb
Mg	0.701 ^a	0.053	0.118	0.315	-0.127	-0.121	0.169	-0.142	-0.553	-0.612	0.071	-0.582	0.624
Al	0.053	0.521 ^a	-0.472	-0.303	-0.525	0.034	-0.323	0.521	0.385	-0.377	0.251	0.278	0.010
K	0.118	-0.472	0.817 ^a	0.041	0.066	-0.150	0.413	0.040	-0.350	-0.188	0.028	-0.278	0.056
Cr	0.315	-0.303	0.041	0.702 ^a	0.239	-0.469	-0.140	-0.496	-0.615	0.231	0.147	-0.605	0.148
Mn	-0.127	-0.525	0.066	0.239	0.563 ^a	0.126	0.117	-0.857	-0.215	0.463	-0.238	-0.212	-0.093
Fe	-0.121	0.034	-0.150	-0.469	0.126	0.864 ^a	-0.150	-0.064	-0.116	-0.278	-0.503	0.112	0.184
Ni	0.169	-0.323	0.413	-0.140	0.117	-0.150	0.753 ^a	0.026	0.013	-0.283	-0.008	-0.156	0.161
Co	-0.142	0.521	0.040	-0.496	-0.857	-0.064	0.026	0.654 ^a	0.378	-0.436	0.166	0.424	-0.022
Cu	-0.553	0.385	-0.350	-0.615	-0.215	-0.116	0.013	0.378	0.583 ^a	0.247	0.262	0.712	-0.543
Zn	-0.612	-0.377	-0.188	0.231	0.463	-0.278	-0.283	-0.436	0.247	0.695 ^a	0.082	0.174	-0.633
Cd	0.071	0.251	0.028	0.147	-0.238	-0.503	-0.008	0.166	0.262	0.082	0.587 ^a	-0.210	-0.556
In	-0.582	0.278	-0.278	-0.605	-0.212	0.112	-0.156	0.424	0.712	0.174	-0.210	0.331 ^a	-0.316
Pb	0.624	0.010	0.056	0.148	-0.093	0.184	0.161	-0.022	-0.543	-0.633	-0.556	-0.316	0.481 ^a

^a - Measures of Sampling Adequacy (MSA)

The two-dimensional representation of the PCA scores (Fig. 12) facilitates the identification of the internal structure of the data and the detection of possible groupings or

differentiations between samples. The significant values for the formation of components within the PCA analysis (shown in Table 11) must be $\geq 0.4 - 0.5$ [26].

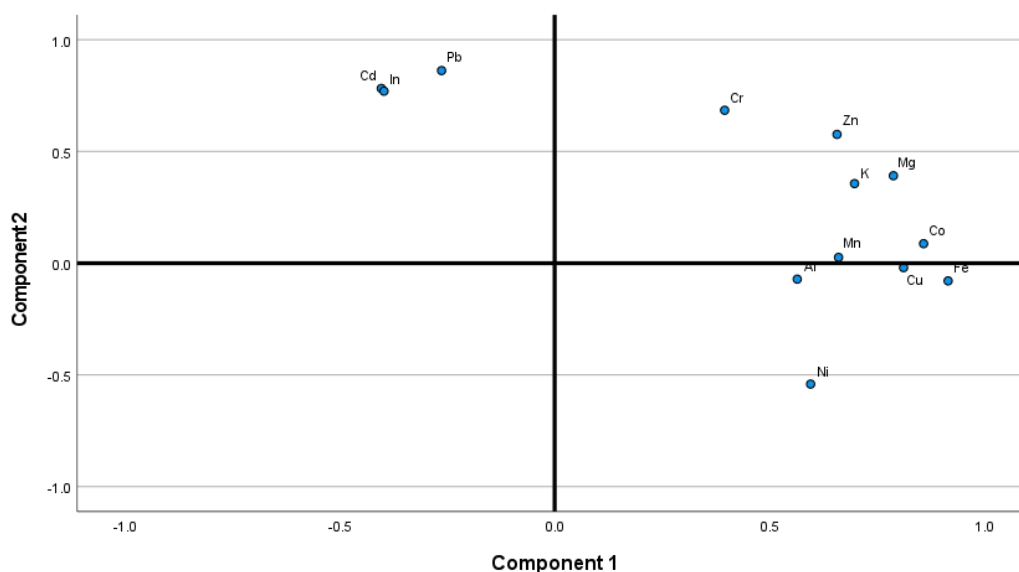


Figure 12. Two-dimensional representation of PCA scores for determined elements in ceramic pigments

Table 11. Principal component analysis of the 13 elements identified in pigment samples.

Elements	Component	
	1	2
Cd	-0.074	0.234
In	-0.073	0.230
Co	0.158	0.026
Cu	0.150	-0.006
Pb	-0.048	0.258
Zn	0.121	0.173
Cr	0.073	0.205
Ni	0.110	-0.162
Mn	0.122	0.008
K	0.128	0.107
Mg	0.145	0.117
Fe	0.169	-0.024
Al	0.104	-0.021

The correlations between these elements can be explained by the thermal treatments to which the clay samples were subjected or by the processing and firing method. The clustering of only three elements for the two components can be explained by: (i) the use of materials with a high load of chemical elements; (ii) the specificity of pigments with a high load of heavy metals; and (iii) the side effects of the firing process or natural variations. However, it is interesting the fact that indium is in the cluster with cadmium and lead. Indium is naturally present in clay and associated with organic matter and iron oxides, while the behavior of cadmium and lead is influenced by the iron oxides (especially by the co-precipitation and absorption of Cd and Pb by the Fe_xO_y) [27].

To validate these observations regarding the PCA analysis, hierarchical cluster analysis was also applied as a complementary analysis. To identify the natural groupings and links between the 20 pottery samples and the 4 soil samples analyzed, cluster analysis was also performed (Fig. 13). This analysis allows the grouping of samples based on elemental composition. Correlation analysis (Fig. 14) aims to investigate the existence and intensity of linear relationships between two numerical variables [28].

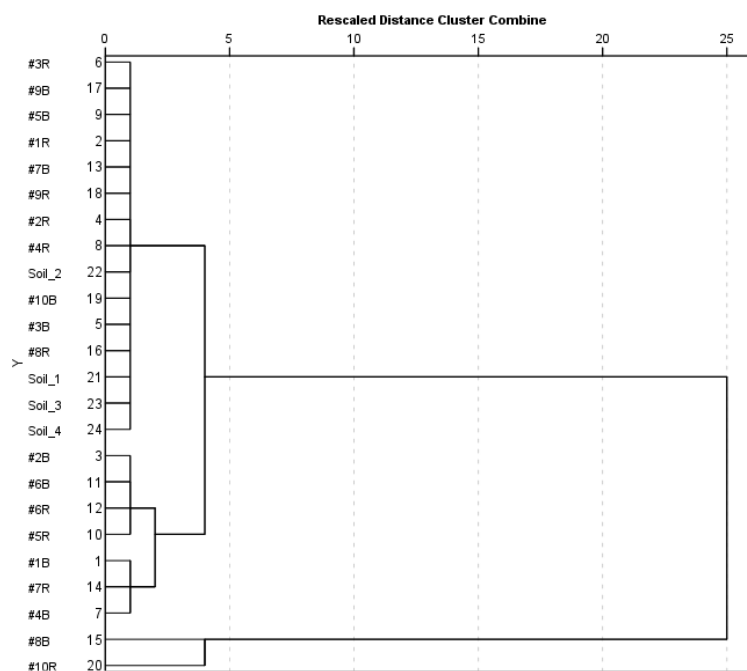


Figure 13. Hierarchical structure of groups for ceramic and soil samples, according to Cluster analysis (Dendrogram using Average Linkage Between Groups)

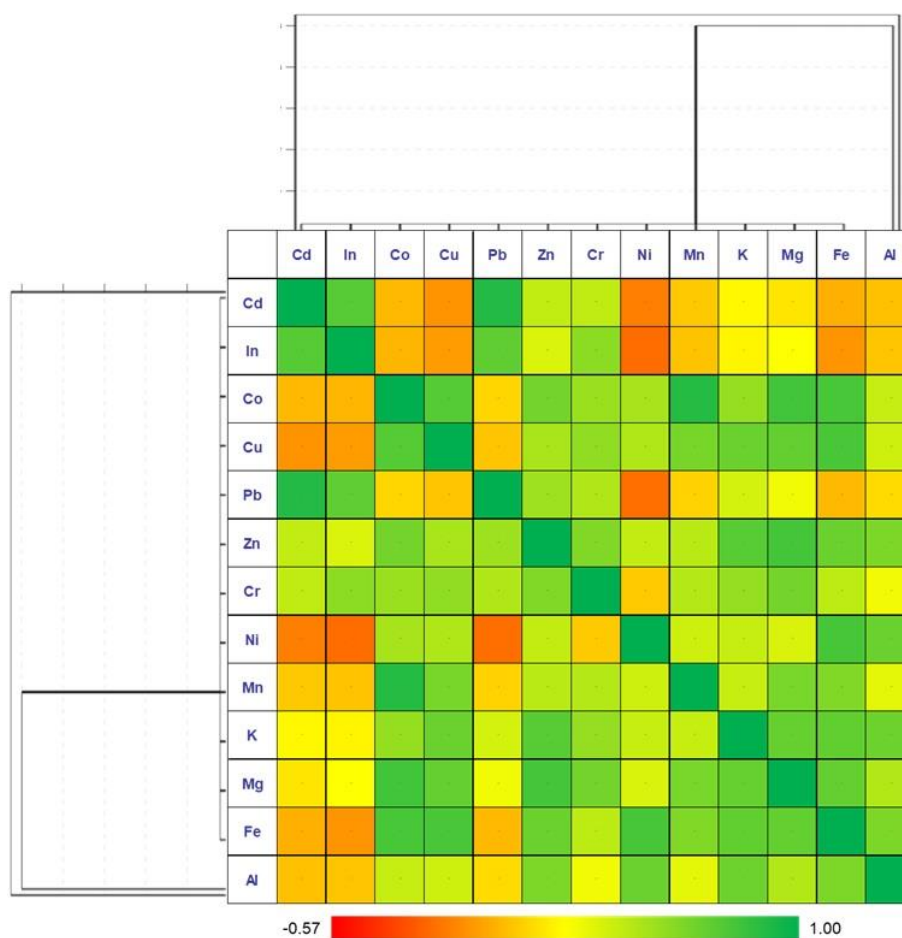


Figure 14. Pearson correlation matrix vs. dendrograms (distribution of correlations between chemical elements in pottery).

The dendrogram obtained highlights four clusters, which can also be considered two major clusters: the first and most loaded cluster is dominated by 11 pottery subsamples (i.e., #3R, #9B, #5B, #1R, #7B, #9R, #2R, #4R, #10B, #3B, #8R) and all soil samples, while other 7 pottery subsamples were integrated into the second cluster, with two pottery subsamples (i.e., #8B and #10R) remained out of those 2 major clusters. The integration of soil samples into the same clusters as the analyzed ceramic samples suggests the use of those soils as a main component in obtaining of the pottery (made from local clay). However, the value of average linkage between groups (i.e., <5%) suggests that between the samples of the first cluster and those from the second one exist a correlation from chemical point of view. The partial overlap between the clusters identified by PCA analysis and those obtained by Cluster Analysis supports the hypothesis of the existence of compositional differences between some subsamples and the raw materials.

In the present study, correlation analysis was applied to investigate the correlations between the chemical elements identified in the pottery subamples. The Pearson correlation coefficient is an indicator that measures the degree of correlation between two variables, and the value of the Pearson correlation coefficient varies between -1 and +1 [29, 30]. Values ≤ 1 indicate a strong correlation, values close to -1 indicate a strong but negative correlation, while values close to 0 suggest the lack of a correlation [30, 31].

Pearson correlation analysis shows strong and significant links between several elements. Significant and strong relationships can be observed between Cd with Pb, but also between Co and Mn, where $r = 0.860$ and $p < 0.001$, and between Cu and Fe ($r = 0.720$, $p < 0.001$). Strong negative correlations with $r < -0.5$ were also identified (example: Cd with Ni or In with Ni). The fact that correlations between only two elements may indicate the intentional addition of those elements in the final composition of the ceramics or an accidental contamination, but neither the technological process nor the heat treatment of obtaining the heritage objects can be excluded.

4. CONCLUSIONS

So-called Herpály painted pottery was produced locally by the Neolithic community from Zăuan-Dâmbul Spânzurașilor. Bitumen or birch bark tar could not be identified in the black pigment subsamples because the IR spectra do not present the specific absorption bands (reported in another study [9]). Considering the iron and manganese content (determined by ICP-MS), it can be concluded that the painting ornaments were applied on the vessels using a local soil characterized by a high content of these elements. Probably, this is the main reason for the fact that the black colour was not well preserved – a bad quality of the pigment and/or an inappropriate painting technique. Another characteristic of the studied ceramic artefacts is the firing temperature lower than 600°C, which can also be a cause for the damaged black paintings. This technological approach of ceramic production by the Neolithic community from Zăuan can explain partially the quality of local pottery.

In addition, it was noticed that from the archaeometric point of view, no differences can be observed between the pottery designated as grave goods and everyday used vessels by the Neolithic community from Zăuan – Dâmbul Spânzurașilor.

REFERENCES

- [1] Lazarovici, G., Lakó, E., Săpăturile de la Zăuan. Campania 1980 și importanța acestor descoperiri pentru neoliticul din N-V României, *Acta Musei Napocensis*, **XVIII**, 26, 1981.
- [2] Băcuet Crișan, S., *Neoliticul și eneoliticul timpuriu în depresiunea Șimleului*, Editura Altip, Sibiu, 2008, p. 41.
- [3] Băcuet Crișan, S., Suplac, Zau, Pișcolt, Herpaly...realitate sau probleme de interpretare?, *Acta Musei Porolissensis*, **XXXV**, 11, 2013.
- [4] Băcuet-Crișan, S., Băcuet-Crișan, D., Pop, D., Mișca, S., Cardoso, R., Ardelean, M., Zoltan, K., Gheorghe, O., Boeru, P., M., Costea, S., Zăuan, com. Ip, jud. Sălaj în *Cronica Cercetărilor Arheologice din România. Campania 2021*, Oradea, 2022, pp. 772-774.
- [5] Băcuet Crișan, S., Gheorghe, O., Kadas Z., Descoperiri funerare din așezarea eneolitică de la Zăuan Dâmbul spânzuraților (Jud. Sălaj). In Colesniuc, S., Talmațchi, G., Dumitrașcu, L.P., Talmațchi, C., *Porți deschise către Civilizații Tomis – Constanța MMXXII, Centenarul Încoronării*, Ed. Mega, Cluj-Napoca, 2022, pp. 71-79.
- [6] Miklos, K., Contribuții noi la cercetarea arheologică a satului Zăuan (jud. Sălaj), *Acta Musei Porolisensis*, **II**, 1978, pp. 17-28.
- [7] Lákó, E., *Raport de cercetare arheologică efectuată la așezarea neolitică de la Zăuan (jud. Sălaj)*, 1978, pp. 11-16.
- [8] Băcuet Crișan, D., Băcuet Crișan, S., Bejinariu, I., Pop, H., Cociș, H., Deac, D., *100 de ani de cercetări arheologice în Sălaj (1918-2018)*, Ed. Mega & Ed. Porolissum, Cluj-Napoca, 2018, p. 16.
- [9] Popescu, P.G., Enache-Preoteasa, C., Badea, F.D., Pripon, E., Maganu, M., *Revista de Chimie*, **63**(5), 470, 2012.
- [10] Carstea (Elekes), A., Gligor, M., Bucurica, I.A., Dulama, I.D., Radulescu, C., Stirbescu, R.M., Stanescu, S.G., Gheboianu, A.I., *Journal of Science and Arts*, **24**(3), 705, 2024.
- [11] Bucurica, I.A., Dulama, I.D., Radulescu, C., Banica, A.L., Stanescu, S.G., *Journal of Fungi*, **10**(12), 844, 2024.
- [12] Filip, D.D., Gligor, M., Lascu, I.A., Bucurica, I.A., Radulescu, C., Stirbescu, R.M., Dulama, I.D., *Romanian Reports in Physics*, **77**(2), 803, 2025.
- [13] Tomus (Szabo), D.E., Gligor, M., Dulama, I.D., Radulescu, C., Bucurica, I.A., Stanescu, S.G., Stirbescu, R.M., *Journal of Science and Arts*, **21**(1), 285, 2021.
- [14] Bintintan, A., Gligor, M., Radulescu, C., Dulama, I.D., Olteanu, R.L., Teodorescu, S., Stirbescu, R.M., Bucurica, I.A., *Analytical Letters*, **52**(15), 2348, 2019.
- [15] Bintintan, A., Gligor, M., Dulama, I.D., Radulescu, C., Stihi, C., Ion, R.M., Teodorescu, S., Stirbescu, R.M., Bucurica, I.A., Pehoiu, G., *Romanian Journal of Physics*, **64**(5-6), 903, 2019.
- [16] Bintintan, A., Gligor, M., Dulama, I.D., Teodorescu, S., Stirbescu, R.M., Radulescu, C., *Revista de Chimie*, **68**(4), 847, 2017.
- [17] Tamilarasi, A., Chandrasekaran, A., *Vibrational Spectroscopy*, **128**, 103584, 2023.
- [18] Yan, B., Liu, S., Chastain, M.L., Yang, S., Chen, J., *Scientific Reports*, **11**, 3316, 2021.
- [19] Egoles, C.P., Medupin, R.O., Nzebuka, G.C., Nnodum, N.A., Ochize, U.P., Eterigho-Ikelegbe, O., Wilson, U.N., Yoro, K.O., *Results in Materials*, **23**, 100584, 2024.
- [20] Velraj, G., Janaki, K., Mohamed Musthafa, A., Palanivel, R., *Spectrochimica Acta Part A: Molecular and Biomolecular Spectroscopy*, **72**(4), 730, 2009.
- [21] Velraj, G., Tamilarasu, S., Ramya, R., *Materials Today: Proceedings*, **2**(3), 934, 2015.
- [22] Ho, J.W.I., Quinn, P.S. *Journal of Archaeological Science: Reports*, **37**, 102945, 2021.

- [23] Shoval, S., Gilboa, A., *Journal of Archaeological Science: Reports*, **7**, 472, 2016.
- [24] Kaiser, H.F., *Psychometrika*, **39**(1), 31, 1974.
- [25] David, C.C., Jacobs, D.J., *Methods in Molecular Biology*, **1084**, 193, 2014.
- [26] Fransen, H., May, A.M., Stricker, M.D., Boer, J., Henni, C., Rosseel, Y., Ocke, M., Peeters, P.H.M., Beulens, J.W.J., *Journal of Nutrition*, **144**(8), 1274, 2014.
- [27] Ketrot, D., Suddhiprakarn, A., Kheoruenromne, I., Singh, B., *Thai Journal of Agricultural Science*, **46**(3), 109, 2013.
- [28] Schober, P., Boer, C., Schwarte, L.A., *Anesthesia and Analgesia*, **126**(5), 1, 2018.
- [29] Akoglu, H., *Turkish Journal of Emergency Medicine*, **18**(3), 91, 2018.
- [30] Ratner, B., *Journal of Targeting, Measurement and Analysis for Marketing*, **17**, 139, 2009.
- [31] Schober, P., Boer, C., Schwarte, L.A., *Anesthesia and Analgesia*, **126**(5), 1, 2018.